The search for negative amplitude components in quasi-continuous distributions of relaxation times: the example of ^{1}H magnetization exchange in articular cartilage and hydrated collagen

The search for negative amplitude components in quasi-continuous distributions of relaxation times: the example of ^{1}H magnetization exchange in articular cartilage and hydrated collagen

Paola Fantazzini[1,5]**, Francesca Galassi**[1,6]**, Villiam Bortolotti**[2]**, Robert J S Brown**[3] **and Franco Vittur**[4]

[1] Department of Physics, University of Bologna, Viale Berti Pichat 6/2, 40127 Bologna, Italy
[2] Department of DICAM, University of Bologna, Viale del Risorgimento 2, 40136 Bologna, Italy
[3] 953 West Bonita Avenue, Claremont, CA 91711-4193, USA
[4] Department of Life Sciences, University of Trieste, via Giorgeri 1, 24137, Italy
E-mail: paola.fantazzini@unibo.it

Abstract. When inverting nuclear magnetic resonance relaxation data in order to obtain quasi-continuous distributions of relaxation times for fluids in porous media, it is common practice to impose a non-negative (NN) constraint on the distributions. While this approach can be useful in reducing the effects of data distortion and/or preventing wild oscillations in the distributions, it may give misleading results in the presence of real negative amplitude components. Here, some examples of valid negative components for articular cartilage and hydrated collagen are given. Articular cartilage is a connective tissue, consisting mainly of collagen, proteoglycans and water, which can be considered, in many aspects, as a porous medium. Separate T_1 relaxation data are obtained for low-mobility ('solid') macromolecular ^{1}H and for higher-mobility ('liquid') ^{1}H by the separation of these components in free induction decays, with α denoting the solid/liquid ^{1}H ratio. When quasi-continuous distributions of

---

[5] Author to whom any correspondence should be addressed.
[6] Current address: Mechanical Engineering Department, South Kensington Campus, Imperial College London, Exhibition Road, London SW7 2AZ, UK.

relaxation times (T_1) of the solid and liquid signal components of cartilage or collagen are computed from experimental relaxation data without imposing the usual NN constraint, valid negative peaks may appear. The features of the distributions, in particular negative peaks, and the fact that peaks at longer times for macromolecular and water protons are at essentially the same T_1, are interpreted as the result of a magnetization exchange between these two spin pools. For the only-slightly-hydrated collagen samples, with $\alpha > 1$, the exchange leads to small negative peaks at short T_1 times for the macromolecular component. However, for the cartilage, with substantial hydration or for a strongly hydrated collagen sample, both with $\alpha \ll 1$, the behavior is reversed, with a negative peak for water at short times. The validity of a negative peak may be accepted (dismissed) by a high (low) cost of NN in error of fit. Computed distributions for simulated data using observed signal-to-noise ratios also verify the need for some negative components. Observed relaxation times and signal ratios can be fitted formally by a simple two-site exchange model that gives the exchange times and the uncoupled relaxation times of the liquid and solid components, with significant trends of these parameters with increasing ^{1}H ratio, α. The solid-to-liquid exchange times are found to be in the range from 10 ms to a few tens of ms at all hydration levels. The results may be of interest for the application of magnetization exchange contrast in the imaging of articular cartilage to determine changes associated with pathologies and ageing. Other important porous media exist where exchange phenomena and negative relaxation components cannot be disregarded.

Contents

1. Introduction

1.1. Quasi-continuous distributions of nuclear magnetic resonance relaxation times and the non-negative constraint

It is common practice in nuclear magnetic resonance (NMR) studies of fluids in porous media to look for positive quasi-continuous distributions of relaxation times to account for multi-component exponential relaxation, often interpreted in terms of 'pore-size' distributions. The occurrence of negative amplitude components is usually not supposed to have any physical meaning. It can be due to computation artefacts or data distortion, and as such they must be prevented. This is done by imposing a non-negative (NN) constraint on the computation, which also serves to prevent wild oscillations in distributions, where an unnecessary but permissible high point may be almost cancelled by a nearby negative point when NN is not applied.

Hence, the NN constraint is usually applied on physical grounds by considering the NMR signal as a linear combination of a number of exponential decays with positive amplitudes. However, there are physical conditions in which decays with negative amplitudes do exist, and the application of the NN constraint not only gives false results, but also causes loss of information about the system under investigation.

In this paper, examples will be given of components with negative amplitudes appearing in relaxation time distributions of ^1H, when at least two pools of nuclei exchange magnetization in such systems as articular cartilage or collagen.

1.2. Cartilage, collagen and NMR

Articular cartilage is a thin tissue at the end of all the diarthrodial joints in the human body, the primary function of which is to minimize the stresses due to joint loading. Cartilage is made of chondrocytes incorporated into an extracellular porous matrix that is composed mainly of water (80% by weight), collagen II fibrils and a small fraction of proteoglycans. As such, it can be considered as a porous medium saturated with water. Collagen fibers give the tissue tensile strength and hinder the expansion of the small fraction of viscoelastic proteoglycan molecules, which provide compressive stiffness.

The goal of many studies of cartilage is to determine the relationships between the composition, structure and material properties of healthy cartilage, and to determine changes associated with pathologies and ageing. For many years NMR has proven to be a valuable technique for the investigation of collagen [1–7] and cartilage, both *in vivo* and *in vitro* [8–12]. In particular, magnetic resonance imaging (MRI) has been firmly established as a non-invasive imaging technique for studies of articular cartilage [8, 12] and collagen [4] by exploiting magnetization transfer (MT) or magnetization transfer contrast (MTC) [13–15].

After the milestone paper of Edzes and Samulsky [1], the magnetization exchange between macromolecular and water protons in hydrated collagen was established and further investigated by the so-called Edzes and Samulsky method [1–3]. Collagen and water ^1H pools can be distinguished through free induction decay (FID). Protons in the 'rigid' matrix contribute to the fast relaxing signal (T_2 of the order of $10\,\mu s$), well separable from the more slowly relaxing signal of the water protons.

The magnetization exchange between the macromolecular and water proton pools was observed *in vivo* using the NMR saturation transfer method by Balaban and Wolff [14, 15]. They observed a decrease in the steady-state magnetization and relaxation times of the water

protons with radio-frequency irradiation of macromolecular protons, and demonstrated that this exchange is tissue specific, giving rise to the new contrast editing MTC in NMR and MRI. Samples of articular cartilage were analyzed *in vitro* after removing proteoglycans, and it was concluded that the structure and concentration of the collagen are the predominant factors affecting magnetization exchange, with a negligible contribution from proteoglycans [8]. In [6], the results led the authors to conclude that an exchange of protons between the protein and the water molecules is the most significant process for MT above the freezing point. In an agar gel model, MTC experiments were performed [16] by varying the off-set frequency, amplitude of radio-frequency irradiation and gel concentration. The authors concluded that the liquid pool has a Lorentzian line shape and the 'semisolid' a Gaussian line shape, with a T_2 of 13 μs. They found that the simple off-resonance irradiation technique has limitations in its ability to saturate the solid-like pool without directly affecting the liquid one. In a study of the MT in human cartilage *in vitro*, a high-power pulse spectrometer was used that is capable of detecting signals from both solid-like and liquid-like protons, and it was concluded that the use of pulse methods to generate MTC is in some cases preferable over steady-state saturation methods [9].

There are different ways of performing experiments on magnetization exchange [17]. In particular, the Goldman–Shen [18] and Edzes–Samulsky [1–3] methods measure the recovery of longitudinal magnetization after a radio-frequency pulse sequence is utilized to disturb either mobile or immobile proton pools. Quantitative imaging of MT has been obtained by using selective pulses [19–22].

In this paper, the Edzes–Samulsky method has been applied to articular cartilage and collagen at different hydration levels. A simple two-site exchange model has proved to be valuable for describing, at least to first approximation, the magnetization exchange mechanism and for evaluating MT parameters.

2. Materials and methods

2.1. Cartilage and hydrated collagen

Cylindrical plugs (7 mm diameter and 1–2 mm thick) of articular cartilage were dissected from the proximal end of the humerus of pigs and maintained in a sterile saline solution. Thin slices of the same tissue were extracted using 4 M guanidinium chloride in 50 mM acetate, pH 7.4 (5 ml g^{-1} of wet tissue) for 72 h under continuous stirring. The rinsed residue of the extraction was used as the collagen type II purified sample. The extraction medium was dialyzed exhaustively against pure water, and this was used as the soluble proteoglycan fraction. Type II collagen and proteoglycans were then lyophilized and stored under dry conditions.

Cartilage samples were obtained by stacking three to four thin plugs inside the NMR glass tube (10 mm external diameter). Four samples were of fresh cartilage; one of these was measured again after drying and one sample was measured at normal temperature after long-time freezing. Three samples were also measured after treatment with 4 M guanidinium, as described above.

Twenty collagen samples were measured at different hydration levels. To obtain these samples, lyophilized collagen II was cut with a scalpel into small pieces and then added at the bottom of the NMR tube to completely fill the sensitive volume; then it was pumped in vacuum for 24 h to remove water. The sample measured in this condition corresponds to the driest (highest solid/liquid ^{1}H ratio, α).

Then, four samples were obtained through the simple contact of the samples with the atmosphere of the laboratory for up to 10 days, at a constant temperature of 23 °C. A more controlled range of hydration was obtained by the contact of one sample with the water vapor of a sequence of six saline solutions at different salt concentrations and temperatures (23, 30 or 37 °C). In the end, two samples with the highest hydration were obtained by absorption of distilled water drops.

2.2. NMR data acquisition

NMR data were acquired at 20 MHz (0.47 T) and 25 °C by a homemade relaxometer equipped with a SPINMASTER console (Stelar, Mede, Italy). The Edzes and Samulsky method consists essentially of the acquisition and, in particular, processing of FIDs (see later) of an inversion recovery (IR) sequence (π-t_i-$\pi/2$ FID acquisition) at variable interpulse delays, t_i. The length of the π pulse (7.2 μs) was chosen to be short enough so that both macromolecular and water magnetizations were inverted simultaneously. For each of the 128 or 64 values of t_i (chosen in geometrical progression from 0.5 ms or less to a time long enough to completely cover the longitudinal relaxation curve, depending on the degree of hydration), the FID was acquired for about 0.25 ms with time points at 0.5–2 μs intervals, starting at 11 μs after the end of the $\pi/2$ pulse.

2.3. Two-spin-pool FID analysis

Almost all the FIDs, obtained at different t_i values, showed the presence of two ^{1}H spin groups, distinguishable on the basis of their different decay shapes: quasi-Gaussian (fast decay, solid-like) and exponential decay (slower decay, liquid-like). In principle, the different behaviors can be ascribed to their different (^{1}H or molecular) mobilities. The algorithm to be applied to analyze the FIDs in the presence of these two ^{1}H populations in biological (bone, collagen and wood) [7, 23] and non-biological samples [24, 25] was decided on in course of time.

Each FID was fitted to the equation

$$S(t) = X_2 \exp\left\{\left[-\tfrac{1}{2}G_{\text{frac}}(t/T_g)^2\right] \times \left[1 - \tfrac{1}{2}(1 - G_{\text{frac}})(t/T_g)^2 \right.\right.$$
$$\left.\left. + \tfrac{1}{4}C_c(1 - G_{\text{frac}})^2(t/T_g)^4\right]\right\} + X_1 \exp(-t/T_{2\text{FID}}), \tag{1}$$

where the first term is assumed to represent the ^{1}H of the solid, and the second term that of the liquid. X_2 is the extrapolated total solid signal and X_1 that of the liquid. G_{frac} is the fraction of the initial curvature of log-FID that is from the Gaussian factor. If $G_{\text{frac}} = 1$, the fit to the solid is Gaussian, as is often used, with a Gaussian decay time T_g. If $G_{\text{frac}} < 1$ the solid part of the fit to the FID has an undershoot (Pake line shape characteristic) or negative excursion. The dimensionless parameter C_c shortens the negative excursion. $T_{2\text{FID}}$ is the T_2 corresponding to the slope of the fitted exponential decay of the liquid. This fit was chosen after fitting stacks of large numbers of FIDs to various expressions, including ones involving Gaussian and sinc functions [23]. Special attention has been devoted to reducing the introduction of scatter in the computed results, by forming stacks of FIDs on which computations were made, and taking into account potential changes in the FID slopes of the liquid component with FID time and with t_i, due to possible T_2 multi-exponential decays. A single value of T_g was used to fit all FIDs of each sequence of FIDs. For each IR sequence, T_g was determined by fitting a stack of FIDs for the first 10 IR times, minus a stack for the last 10. Using the same value of T_g, the

next stacks of 10, each with the last stack subtracted, were fitted to determine the values of $T_{2\text{FID}}$ as a function of IR time. An accurate determination of the two extrapolated FID signal amplitudes at each t_i can be obtained, to produce separate files for the computation of one-dimensional quasi-continuous T_1 distributions for both spin groups. The inversion algorithm (UPEN, for uniform-penalty) [26] uses a regularizing, or smoothing, coefficient that varies with relaxation time and is determined by iterative negative feedback in such a way that the smoothing penalty, rather than the coefficient, is roughly uniform. This can give sharp lines that are not broadened more than is consistent with the noise, and in the same distribution show a tail decades long without breaking it up into several peaks not required by the data to be separate peaks, which might be misinterpreted as physically meaningful resolved compartments. With an appropriate parameter choice from the optional parameters menu, our software UpenWin, which implements the algorithm UPEN, allows the inclusion of negative amplitude components in the relaxation time distribution. UPEN also estimates a root-mean-square (rms) random noise that suppresses the effect of a slowly varying misfit to the data, thereby giving essentially the same value even when the rms misfit (residual) is substantially increased by the application of NN.

Both the liquid and solid parts of the FID signals are extrapolated to zero FID time, as described, and in the T_1 inversion using UpenWin, the signals are extrapolated to zero IR time, giving the solid/liquid signal ratio, α.

2.4. Evaluation of the inversion efficiency

The solid/liquid ratio of the extrapolated signals would give the solid/liquid ^{1}H ratio if the π and $\pi/2$ pulses were fully 'hard'. However, a small correction might be needed because of the fact that some of the solid frequencies deviate from the central frequency by differences that are not negligible with respect to the nutation frequency due to the B_1 field in the rotating frame.

By assuming $T_g = 11$–$12\,\mu$s and the $\pi/2$ pulse width of $3.6\,\mu$s, the acquired solid signal is computed [23] to be reduced by about 5%. The extrapolated solid/liquid signal ratio was divided by a correction factor 0.95, although the correction is small and likely to be comparable to uncertainties in the extrapolations.

2.5. General two-compartment spin exchange

With simple two-site magnetization exchange, one would expect liquid and solid distributions to each have peaks at the same two relaxation times, with the possibility of a peak with small or negative amplitude. In order to test whether the relaxation data were compatible with a simple two-site solid–liquid exchange model, the following algorithm was applied.

Let α be the ratio of the number of ^{1}H spins in pool A (solid) to that in pool B (liquid). At equilibrium, if the residence time in A is τ (reciprocal solid-to-liquid exchange rate), then the residence time in B is τ/α. The exchange rates for A and B are just the reciprocals of the residence times. Let r_a and r_b be the inherent (uncoupled) relaxation rates of A and B, and let r be either of the rates of the coupled system. The equations for the change in polarization (*intensive* variables, a and b, amount of magnetization per amount of hydrogen) in A and B are based on the normal modes, or eigenstates, in which the time derivative operator is replaced by $-r$. Let subscript a refer to the solid (or to the longer coupled T_1 in the case of a second subscript) and b to the liquid (or to the shorter coupled T_1 in the case of a second subscript);

IOP Institute of Physics ⊕ DEUTSCHE PHYSIKALISCHE GESELLSCHAFT

then the exchange is given by

$$-ra = -r_a a + (b-a)/\tau; \quad -rb = -r_b b + (a-b)\alpha/\tau. \tag{2}$$

Each of these two equations can be solved for b/a and these values equated, giving the quadratic equation in $r\tau$,

$$(r\tau)^2 - (r\tau)(r_b\tau + r_a\tau + \alpha + 1) + r_a r_b \tau^2 + \alpha r_a \tau + r_b \tau = 0. \tag{3}$$

There are two roots, $r\tau = c \pm (c^2 - d)^{1/2}$, where $c = (r_b\tau + r_a\tau + \alpha + 1)/2$ and $d = r_a r_b \tau^2 + \alpha r_a \tau + r_b \tau$.

We note that equation (3) has either one or two powers of τ in each term, giving the simple expression,

$$\tau = \frac{\alpha r_a + r_b - (\alpha + 1)r}{(r_a - r)(r - r_b)}. \tag{4}$$

Either of the coupled rates would ideally give the same A → B exchange time, but (4) is likely to be useful mainly in the case of the longer time.

Let f_a be the fraction of the spins in A and f_b that in B. Then $\alpha = f_a/f_b$. Let f_{aa} be the fraction of the A spins in the coupled eigenstate with the longer coupled T_1 (smaller coupled rate) and f_{ab} be the fraction with the shorter coupled T_1. Then $f_{aa} + f_{ab} = 1$. If we designate the two coupled eigenrates as r_{xa} and r_{xb} (x for exchange), we have conservation of initial slope separately in A and B. If A and B have equal initial polarization, such as from *hard* $\pi/2$ pulses, the initial polarizations may be given unit values. Since initial polarizations are equal in A and B, the exchange between A and B does not cause any net flow of magnetization between them at time zero. Thus, the initial slopes are r_a and r_b, with or without coupling, with $f_{aa}r_{xa} + f_{ab}r_{xb} = r_a$, and analogously for B, with $f_{bb} + f_{ba} = 1$ and $f_{ba}r_{xa} + f_{bb}r_{xb} = r_b$. These four equations may be solved for the four f values:

$$f_{aa} = \frac{r_{xb} - r_a}{r_{xb} - r_{xa}}, \quad f_{ab} = \frac{r_a - r_{xa}}{r_{xb} - r_{xa}}, \quad f_{bb} = \frac{r_b - r_{xa}}{r_{xb} - r_{xa}}, \quad f_{ba} = \frac{r_{xb} - r_b}{r_{xb} - r_{xa}}. \tag{5}$$

For data where one can separate solid and liquid signals, one may know r_{xa} and r_{xb} and all f values. One can then, in principle, obtain r_a and r_b and use (4) to obtain τ, the residence time for A. The above expression does not involve τ, but this lack of τ-dependence requires that initial polarizations be the same in A and B. However, in many cases it is not possible to determine the parameters (especially f_{ab} and f_{bb}) well enough to obtain reliable values of r_a and τ.

If the initial polarizations are not equal, as from *soft* pulses (or only marginally hard pulses) in the A phase (here, the solid), the initial polarization is reduced by a factor of P_a, and one obtains $f_{aa}r_{xa} + f_{ab}r_{xb} = r_a - (1-P_a)/\tau_{ab}$ and $f_{ba}r_{ax} + f_{bb}r_{bx} = r_b + (1-P_a)/\tau_{ba}$, where $\tau_{ba} = \tau_{ab}/\alpha$. Therefore, one no longer obtains equations like (4) that do not involve exchange rates. The f values are $f_{aa} = 1 - f_{ab}$ and $f_{bb} = 1 - f_{ba}$, with

$$f_{ab} = \frac{r_a - r_{xa} - (1-P_a)/\tau}{r_{xb} - r_{xa}}, \quad f_{ba} = \frac{r_{xb} - r_b + \alpha(1-P_a)/\tau}{r_{xb} - r_{xa}}. \tag{6}$$

If we consider the two-site exchange model as an approximation for the data, we must consider the usually small differences between the longer solid T_1 and the longer liquid T_1 to be due either to model approximation or experimental error. We have written a search program that
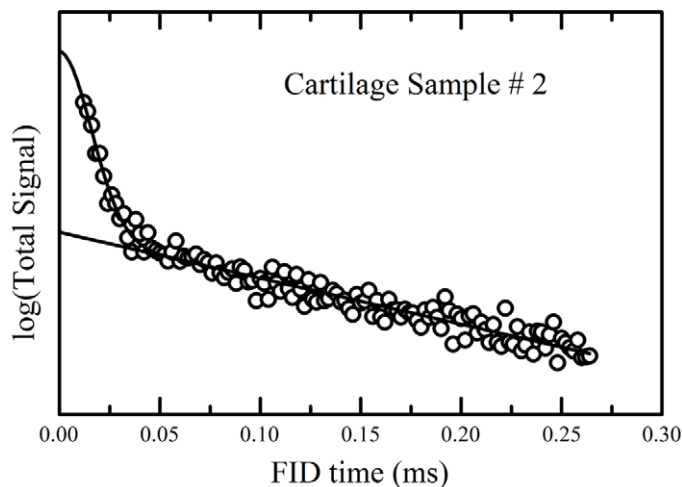
Figure 1. FID obtained in IR measurements on a sample of native articular cartilage (sample 2), with extrapolated liquid and total signals shown on a semi-logarithmic scale. Initial portions of the FIDs show the typical behavior of the low-mobility nuclei of a solid component (almost all collagen protons), and the following slope represents the liquid component (water).

uses the input parameters r_{xa}, r_{xb}, α, f_{ba} and P_a (computed or assumed value). It first obtains r_b from (5) (or (6), if $P_a \neq 0$). Then, an initial value of $T_a = 1/r_a$ just slightly larger than T_{xa} is assumed. Then, a low starting value of τ is used and increased until the input value of r_{xb} is reached. This is then done by increasing the values of T_a until the input value of T_{xa} is reached (or until an excessive value of r_a is reached, indicating that there is no solution). If $T_{aa} \neq T_{ba}$ or a solution cannot be found, presumably the exchange conditions are somewhat more complex than those for the simple two-site model.

3. Results

3.1. Results on cartilage

Native cartilage shows two FID spin pools. FIDs obtained for each recovery time in IR measurements gave a very fast quasi-Gaussian component in the FID, due to ^{1}H nuclei with reduced mobility ('solid'), and a longer-lived exponential due to the liquid. The Gaussian or quasi-Gaussian time T_g was in the range 13–15 μs, with a solid/liquid ratio α in the range 0.1–0.7 (this last value for sample 4 after drying). Figure 1 shows, on a semi-logarithmic scale, the FID and the fitted curve for cartilage sample 2 ($\alpha = 0.12$).

The cartilage samples were measured in the 'fresh' state, after longer times for larger sample numbers, with sample 4 in the dried condition and sample 5 after further drying by freezing. Samples 1–3 were also measured after treatment to remove proteoglycans. Amounts of signal for the liquid component decreased with time and with additional drying. Relaxation rates (reciprocal times) of the liquid components were approximately proportional to α, presumably proportional to the surface-to-volume ratio of the liquid.

3.2. Signs of magnetization exchange between solid and liquid components in the cartilage

As mentioned, with a simple two-site magnetization exchange, one would expect liquid and solid distributions to each have two peaks, at the same two relaxation times, with the possibility of a peak with small or negative amplitude. The signal-to-noise (S/N) ratio for the solid component is very low for the cartilage samples, making the distributions rather wide. Nevertheless, for all the cartilage samples, the major portion of the solid signal is at about the same T_1 as the major liquid component, suggesting the magnetization exchange between the two proton pools.

Moreover, for the two samples with the highest water content (samples 1 and 2) a slight negative peak at about 20 ms is seen for the liquid if the non-negative constraint, NN, is not applied (figures 2(a) and (b)). These two samples give unacceptable errors of fit, as shown in figure 2(c), if the negative components are prevented by allowing the usual NN constraint in the inversion computation. This occurs only for samples 1 and 2, with the lowest α or the highest water content. The signal intensity of this negative peak is very small (about 0.7%), but it is at the same position as a part of the long tail toward shorter times of the corresponding solid signal, which extends well beyond the small shoulder of the liquid peak, as shown for cartilage sample 2 in figure 2(b).

Although it seems clear from the similar T_1 values of the main liquid and solid peaks, and of the liquid negative peak and the part of the tail of the solid peak, that there is magnetization exchange between the solid and the liquid, the shoulder on the liquid peak makes it clear that the system is more complex than that of ideal two-pool exchange. The shoulder on the liquid peak accounts for about 7% of the signal and is at about $T_1 = 130$ ms. This component is also noted by Lattanzio *et al* [11], also at about 130 ms. They find $\alpha = 3.5\%$; thus, their cartilage sample is several times more hydrated than ours.

Ignoring the additional 7% shoulder on the peak for the liquid component, one can use the observed solid/liquid ^{1}H ratio α and a two-exponential-component fit to the T_1 distribution, for the solid to compute exchange times and other parameters. This gives the solid-to-liquid exchange time $\tau = 20$ ms and gives 1.7% for the negative liquid peak, somewhat larger than the observed 0.7% shown in figure 2.

3.3. Signs of magnetization exchange between solid and liquid components in proteoglycans

Measurements made on the proteoglycan-depleted sample 2 gave results very similar to those shown in figure 2.

The behavior shown in figure 3 for a proteoglycan sample also suggests a magnetization exchange between the solid and the liquid. It is worth pointing out that UPEN or other inversion algorithms may give an undershoot between nearby positive peaks if NN is not used, thereby enhancing the peaks by the amount of undershoot. With nearby negative and positive peaks, both may be enhanced by the transition between them. The negative peak in figure 3 is 17% of the total. If we use a two-exponential fit to the liquid to compute exchange parameters, we get the solid–liquid $\tau = 13$ ms and a negative solid component of only 8%.

3.4. Results on collagen hydrated under controlled conditions

The FIDs of collagen samples 1–18, hydrated under controlled conditions and with $\alpha > 2.8$, could be fitted by equation (1), with $T_g = 11.2\,\mu$s, $G_{frac} = 0.55$ and $C_c = 0.25$, with slightly
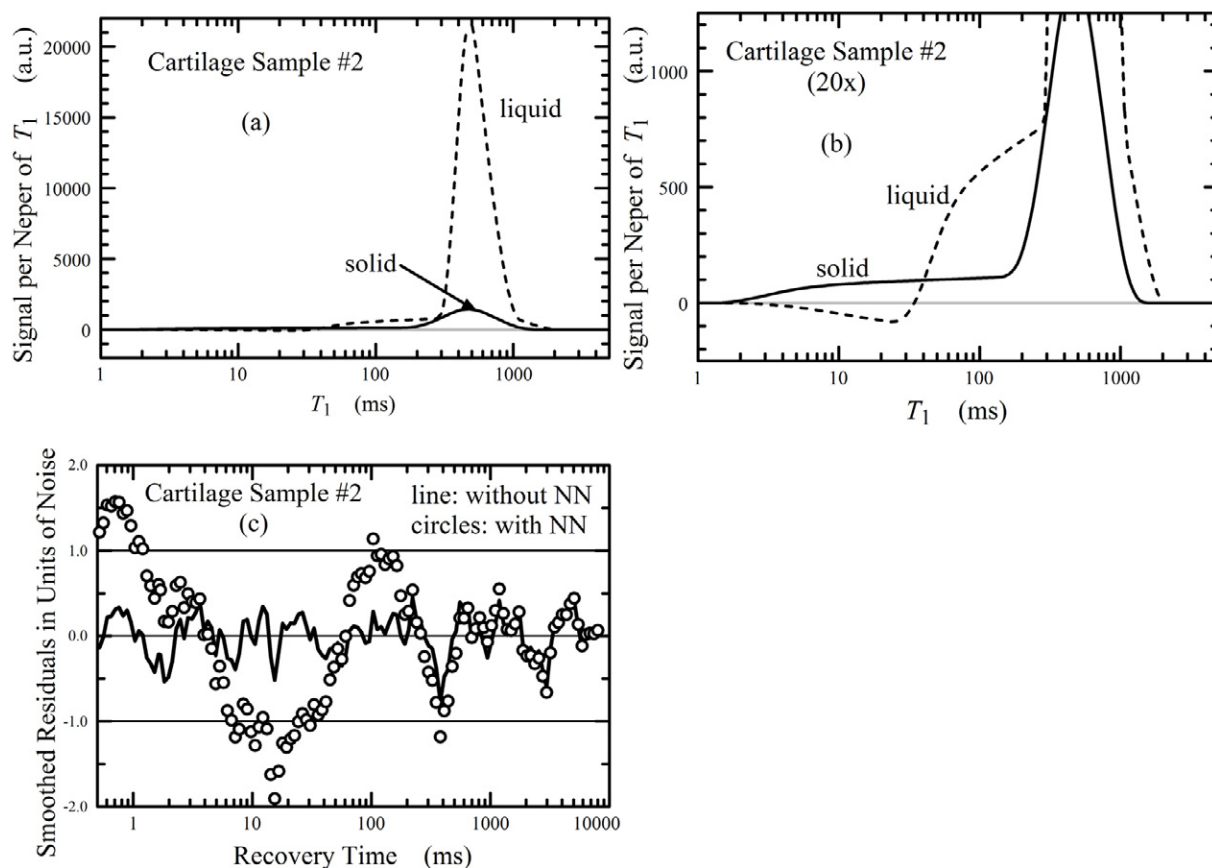
Figure 2. T_1 distributions, shown at $1\times$ (a) and $20\times$ (b), for the solid and liquid FID components for cartilage 2, which has a solid/liquid ^{1}H ratio of $\alpha = 0.12$. Both were inverted with UPEN without NN, the non-negative constraint. The S/N ratio is 1325 for the liquid and 20 for the solid. The residuals, or errors of fit in units of the random noise, are shown for the liquid, inverted both with and without NN, in (c), smoothed by averaging each point with its three neighbors on each side for display purposes. Without NN, the residuals have close to zero mean and appropriate rms scatter (about $7^{-1/2}$ for the averages of seven points). With NN, there are 24 consecutive points, at times near those of the negative peak, with residuals at about -1 or worse, far outside the statistical plausibility for an acceptable fit. The autocorrelation of residuals stops at about 400 ms, where only the long-T_1 component is still present.

different values required for the two more hydrated samples. The solid–liquid separation of the FIDs gave the files of longitudinal relaxation data for the solid and the liquid.

For samples 1–19, T_1 distributions gave two positive peaks (for sample 1 a peak and a long tail to shorter times) for the liquid, with the higher amount of signal in the longer-T_1 peak. For samples 3–19, all but the driest and wettest, the T_1 data show a negative peak for the solid component at about the same T_1 as that of the smaller positive peak of the liquid. The data also show a positive peak for the solid at a longer time, which is about the same as that of the longer-T_1 peak for the liquid. Figure 4 shows T_1 distributions for four collagen examples, corresponding
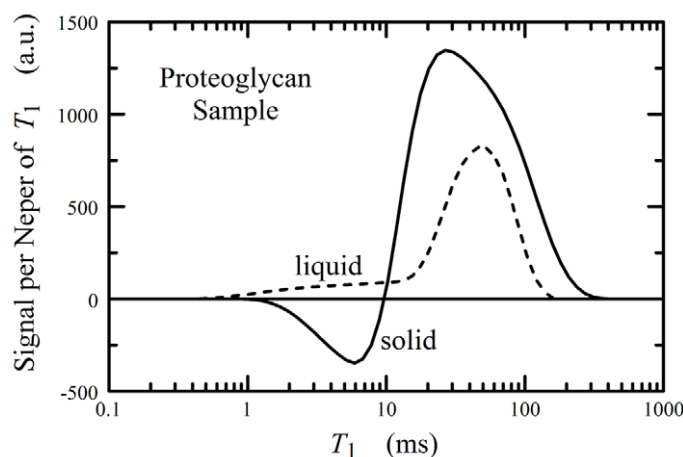
Figure 3. T_1 distributions for a proteoglycan sample. Inversions by UPEN for both solid and liquid were without the NN constraint. The solid/liquid ^{1}H ratio is $\alpha = 1.6$. The low S/N ratio does not yield the resolution of the liquid peaks, but the tail is clearly over the negative solid peak.

to the driest collagen sample (a), an intermediate (b), more hydrated (c) and a strongly hydrated one (d). Sample 20, unlike the less strongly hydrated samples, shows two positive peaks for the solid and a very small negative peak for the liquid, much like that shown in figure 2 for the cartilage. Both these samples have $\alpha \ll 1$, while $\alpha > 1$ for collagen samples 1–19.

The solid curves in figures 4(b) and (c) show negative peaks, descending immediately from large positive peaks. This undershoot increases the amplitude of the negative peak somewhat and also shifts it toward the larger peak, as discussed in connection with figure 3. If we really have a system with two fairly homogeneous exchanging ^{1}H pools, then a simple two-exponential-component computation of relaxation times and amplitudes is more robust than the computation of a quasi-continuous distribution, and avoids the distortion associated with a possible undershoot. Figures 4(b) and (c) show the distributions (open circles) computed from synthetic data using the relaxation times and amplitudes from the two-component fits, with the lines taken as Gaussian with 0.1 Neper half-widths. These fit the real data well, confirming the adequacy of the two-exponential-component fits for these samples.

Two-exponential fits were made to the data for the liquid for each of the samples, and the two relaxation times for the liquid and the value of the percentage of signal in the long-T_1 peak for the liquid (f_{ba}), along with the α from FID analysis, were used in the two-site exchange model to obtain the exchange time from the solid to the liquid (τ), the intrinsic relaxation time for the solid $T_a(=1/r_a)$ and the liquid $T_b(=1/r_b)$, and the percentage with *negative* amplitude of the short component for the solid (f_{ab}). The first five samples (highest α and shortest $T_{2\mathrm{FID}}$) did not give solutions.

The validity of the model of two exchanging pools for the collagen samples is supported by the data for the distributions shown in figure 4(c). Each 'pool' should show the same two relaxation times. The T_1 values computed in two-exponential-component fits to liquid and solid give 61.2 and 11.3 ms for the liquid and 62.0 and 10.2 ms for the solid, even though the 10.2 ms peak for the solid is of negative amplitude.
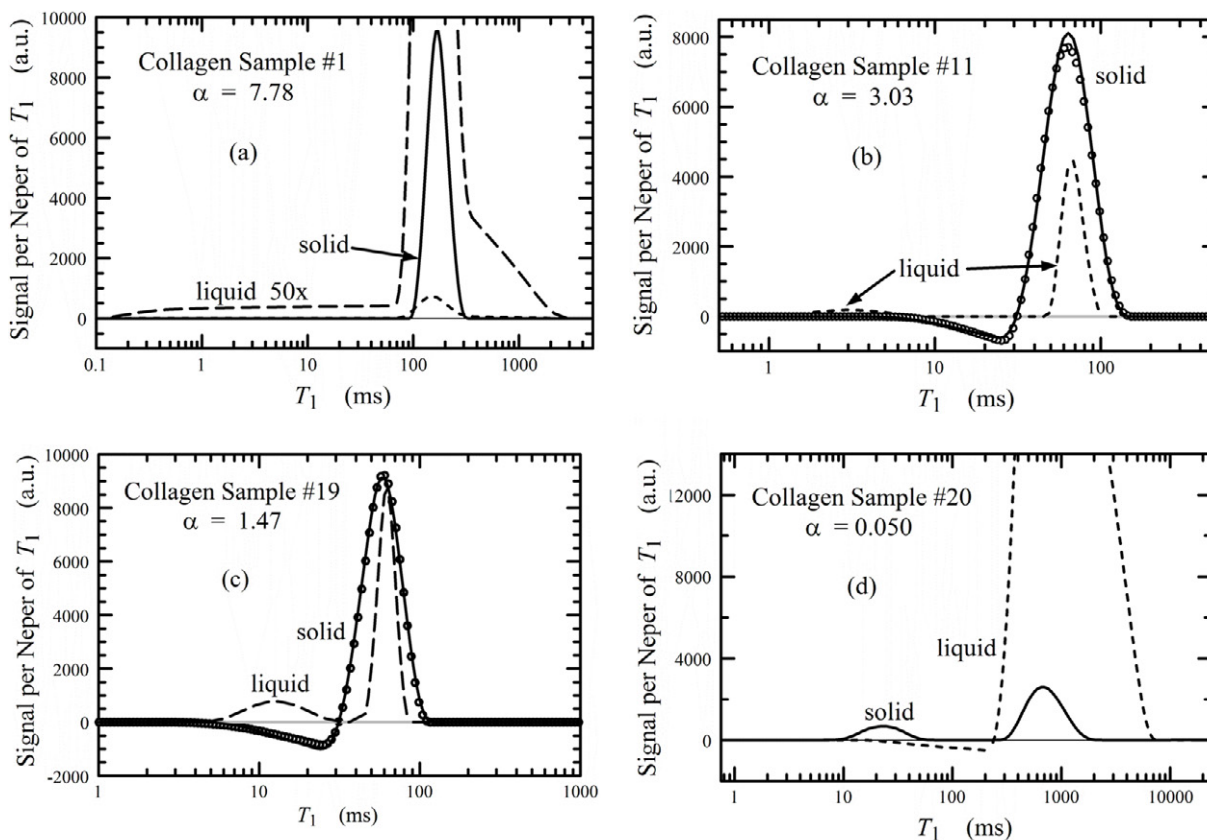
Figure 4. T_1 relaxation time distributions for four representative collagen samples. (a) The driest sample, (b) an intermediate sample, (c) a more hydrated sample, and (d) a strongly hydrated sample. Solid lines are the distributions for the solid and the dashed lines are those for the liquid. Open circles are inverted from synthetic data based on two-exponential-component fits to the data. The NN constraint was applied to distributions that have two positive peaks, with negligible increase in error of fit for (b) and (c) and an acceptably small increase for (d). The application of NN to the data for which negative peaks are shown above, gives completely unacceptable increases in error of fit.

Figure 5 shows the plots of $1/\tau$, r_a, r_b as functions of α. There appears to be somewhat of a trend for $1/\tau$ in figure 5(a) over a limited range of α, but there is no evident reason to expect a linear relationship more than locally. Likewise, the points for r_a in figure 5(b) fall near a line, but there is no reason to expect the solid relaxation rate to go to zero when α is slightly less than 4. On the other hand, the proportionality of r_b (inherent liquid rate) to α is consistent with the idea that the surface-to-volume ratio of the liquid is proportional to α, since α is the ratio of the amount of solid 1H (associated with the surface) to that of the liquid (volume).

4. Discussion and conclusions

When inverting NMR relaxation data in order to get quasi-continuous distributions of relaxation times for fluids in porous media, it is common practice to prevent negative components by imposing a NN constraint on the distributions. While this approach can be useful in reducing
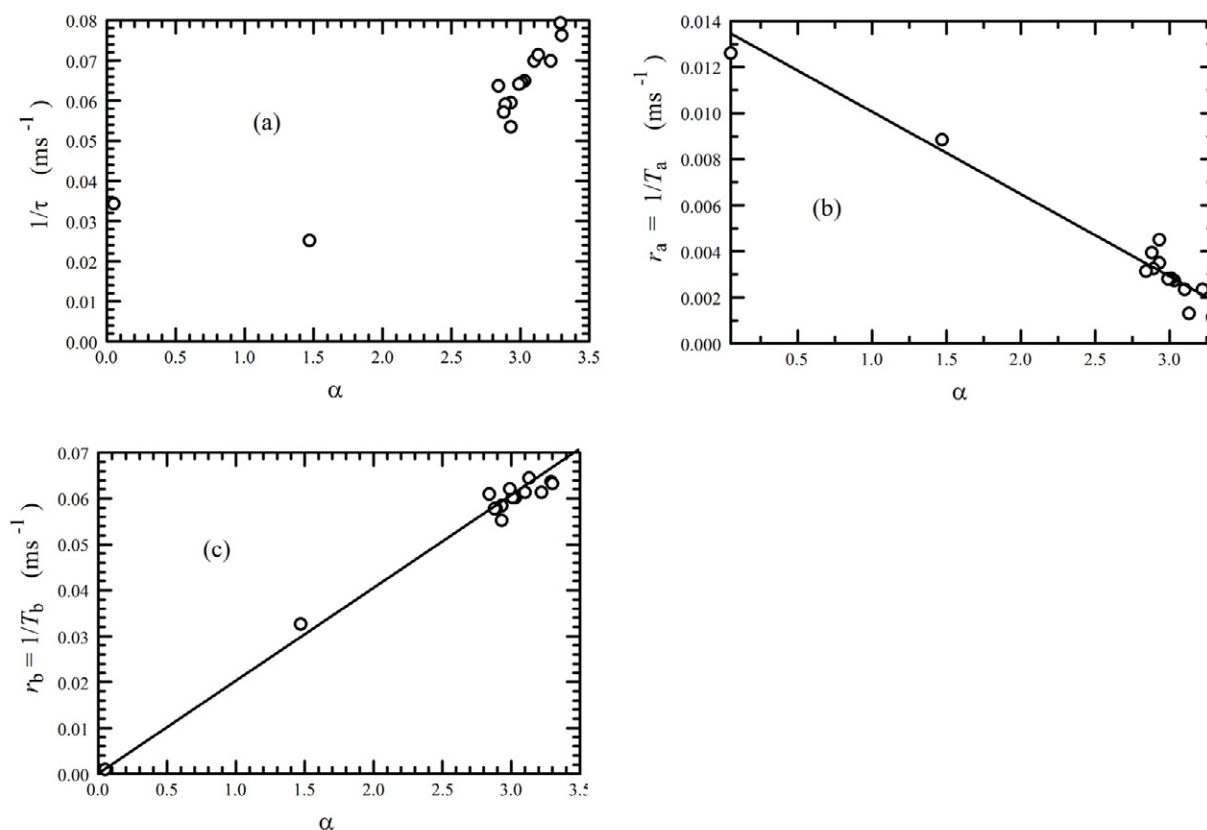
Figure 5. Plots of the results of the two-site spin exchange model for collagen samples, plotted against the solid/liquid ^{1}H ratio, α. Here τ is the computed solid-to-liquid exchange time, T_a is the computed uncoupled (as without exchange) T_1 of the solid, and T_b that of the liquid. Panels (b) and (c) show the surface effects on relaxation, in addition to exchange effects, for both the liquid and the solid.

the effects of data distortion and/or preventing wild oscillations in the distributions, it may give misleading results in the presence of real negative amplitude components, the existence of which is indicated by an unacceptable error of fit if the NN constraint is applied.

In this paper, FIDs were analyzed to give separate solid (macromolecular) and liquid (water) relaxation data from IR T_1 measurements on samples of cartilage, proteoglycans and collagen. The relaxation data were then inverted to obtain distributions of T_1 relaxation times. Many of these distributions showed significant negative peaks when inverted without the usual NN constraint, with unacceptable increases in error of fit if NN was imposed. Synthetic data with corresponding negative components gave similar results.

These negative peaks are presumed to be due to a magnetization exchange between the macromolecular and the water ^{1}H, which, in the simplest case of an ideal two-site exchange, requires that the solid and liquid T_1 distributions each have peaks at the same two relaxation times. This is observed, within experimental error, for the 20 collagen samples and the proteoglycan sample.

Major solid and liquid peaks are also at the same times for the cartilage, which for some samples has a small negative liquid peak at about the same time as part of the solid distribution.

However, the cartilage is clearly not an ideal two-site system, since there is a small second liquid component, shown in figure 2(b) of this paper and noted in [11].

For the samples with the solid/liquid ^{1}H ratio $\alpha > 1$, there are two liquid peaks and a small negative solid peak in addition to the main positive peak. For the cartilage samples and for collagen sample 20, both with $\alpha \ll 1$, there are two solid peaks and a small negative liquid peak in addition to the main positive peak.

These data were used in the computation of two-site exchange and yielded solid-to-liquid exchange times τ in the range from 10 ms to a few tens of ms for all samples, with a slight trend to shorter τ for larger α. The two-site exchange model may be a rough model, because more spin pools could be involved [5, 11] and the relaxation mechanism could be more complicated, but the results give clear indications of the order of magnitude for the parameters involved and of their trends with increasing hydration of the macromolecular component.

Articular cartilage and hydrated collagen have been considered as examples where valid negative components can contribute to the NMR signal. These examples demonstrate the need for careful examination of the data before applying an NN constraint to the distributions. Other porous media in which exchange effects cannot be disregarded do exist, as has been demonstrated in a recent study of the dynamics of water in polyelectrolyte multi-layers [27].

Acknowledgment

References

[1] Edzes H T and Samulski E T 1977 Cross relaxation and spin diffusion in the proton NMR of hydrated collagen *Nature* **265** 521–3

[2] Edzes H T and Samulski E T 1978 The measurement of cross-relaxation effects in the proton NMR spin-lattice relaxation of water in biological systems: hydrated collagen and muscle *J. Magn. Reson.* **31** 207–29

[3] Fung B M and McGaughy T W 1980 Cross relaxation in hydrated collagen *J. Magn. Reson.* **39** 413–20

[4] Harel A, Eliav U, Akselrod S and Navon G 2008 Magnetization transfer based contrast for imaging denatured collagen *J. Magn. Reson. Imaging* **27** 1155–63

[5] Fullerton G D, Nes E, Amurao M, Rahal A, Krasnosselskais L and Cameron I 2006 An NMR method to characterize multiple water compartments on mammalian collagen *Cell Biol. Int.* **30** 66–73

[6] Eliav U and Navon G 2002 Multiple quantum filtered NMR studies of the interaction between collagen and water in the tendon *J. Am. Chem.* S **124** 3126–32

[7] Fantazzini P, Bortolotti V, Brown R J S, Camaiti M, Garavaglia C, Viola R and Giavaresi G 2004 Two 1H-NMR methods to measure internal porosity of bone trabeculae: by solid-liquid signal separation and by longitudinal relaxation *J. Appl. Phys.* **95** 339–43

[8] Kim D K, Cecker T L, Hascall V C, Calabro A and Balaban R S 1993 Analysis of water-macromolecule proton magnetization transfer in articular cartilage *Magn. Reson. Med.* **29** 211–5

[9] Morris G A and Freemont A J 1992 Direct observation of the magnetization exchange dynamics responsible for magnetization transfer contrast in human cartilage *in vitro Magn. Reson. Med.* **28** 97–104

[10] Gray M L, Burstein D, Lesperance L M and Gehrke L 1995 Magnetization transfer in cartilage and its constituent macromolecules *Magn. Reson. Med.* **34** 319–25

[11] Lattanzio P-J, Marshall K W, Damyanovich A Z and Peemoeller H 2000 Macromolecule and water magnetization exchange modeling in articular cartilage *Magn. Reson. Med.* **44** 840–51

[12] Fragonas E, Mlynarik V, Jellus V, Micali F, Piras A, Toffanin R, Rizzo R and Vittur F 1998 Correlation between biochemical composition and magnetic resonance appearance of articular cartilage *Osteoarthritis Cartilage* **6** 24–32

[13] Henkelman R M, Stanisz G J and Graham S J 2001 Magnetization transfer in MRI: a review *NMR Biomed.* **14** 57–64

[14] Balaban R S and Wolff S D 1991 Magnetization transfer contrast and proton relaxation and use thereof in magnetic resonance imaging *United States Patent 5050609*, http://www.freepatentsonline.com/5050609.html

[15] Wolff S D and Balaban R S 1989 Magnetization transfer contrast (MTC) and tissue water proton relaxation *in vivo Magn. Reson. Med.* **10** 135–44

[16] Henkelman R M, Huang X, Xiang Q-S, Stanisz G J, Swanson S D and Bronskill M J 1993 Quantitative interpretation of magnetization transfer *Magn. Reson. Med.* **29** 759–66

[17] Hua J and Hurst G C 1994 Analysis of on- and off-resonance magnetization transfer techniques *J. Magn. Reson. Imaging* **5** 113–20

[18] Goldman M and Shen L 1966 Spin-spin relaxation in LaF_3 *Phys. Rev.* **144** 321–31

[19] Gochberg D F, Kennan R P and Gore J C 1997 Quantitative studies of magnetization transfer by selective excitation and T_1 recovery *Magn. Reson. Med.* **38** 224–31

[20] Gochberg D F, Kennan R P, Robson M D and Gore J C 1999 Quantitative imaging of magnetization transfer using multiple selective pulses *Magn. Reson. Med.* **41** 1065–72

[21] Gochberg D F and Gore J C 2003 Quantitative imaging of magnetization transfer using an inversion recovery sequence *Magn. Reson. Med.* **49** 501–5

[22] Gochberg D F and Gore J C 2007 Quantitative magnetization transfer imaging using via selective inversion recovery with short repetition times *Magn. Reson. Med.* **57** 437–41

[23] Fantazzini P, Maccotta A, Gombia M, Garavaglia C, Brown R J S and Brai M 2006 Solid–liquid NMR relaxation and signal amplitude relationships with ranking of seasoned softwoods and hardwoods *J. Appl. Phys.* **100** 0749071–77

[24] Gombia M, Bortolotti V, De Carlo B, Mongiorgi R, Zanna S and Fantazzini P 2010 Nanopore structure buildup during endodontic cement hydration studied by time-domain nuclear magnetic resonance of lower and higher mobility [1]H *J. Phys. Chem.* B **114** 1767–74

[25] Gombia M, Bortolotti V, Brown R J S, Camaiti M, Cavallero L and Fantazzini P 2009 Water vapor absorption in porous media polluted by calcium nitrate studied by time domain nuclear magnetic resonance *J. Phys. Chem.* B **113** 10580–6

[26] Fantazzini P and Brown R J S 2005 Units in distributions of relaxation times *Concepts Magn. Reson.* **27A** 122–3

[27] Wende C and Schönhoff M 2010 Dynamics of water in Polyelectrolyte multilayers: restricted diffusion and cross-relaxation *Langmuir* **26** 8352–7